Multiresonator quantum memory

S. A. Moiseev,[1,2,*] F. F. Gubaidullin,[2] R. S. Kirillov,[3] R. R. Latypov,[3] N. S. Perminov,[1,2]
K. V. Petrovnin,[3] and O. N. Sherstyukov[3]

[1]*Kazan Quantum Center, Kazan National Research Technical University named after A.N. Tupolev, 10 K. Marx Street, Kazan 420111, Russia*

[2]*Zavoisky Physical-Technical Institute of the Russian Academy of Sciences, 10/7 Sibirsky Tract, Kazan 420029, Russia*

[3]*Kazan Federal University, 18 Kremlyovskaya Street, Kazan 420008, Russia*

(Received 17 September 2016; published 30 January 2017)

In this paper we present universal broadband multiresonator quantum memory based on the spatial-frequency combs of the microresonators coupled with a common waveguide. We find a Bragg-type impedance matching condition for the coupling of the microresonators with a waveguide field that provides an efficient broadband quantum storage. The analytical solution obtained for the microresonator fields enables sustainable parametric control of all the memory characteristics. We also construct an experimental prototype of the studied quantum memory in the microwave spectral range that demonstrates basic properties of the microwave microresonators, their coupling with a common waveguide, and independent control of the microresonator frequencies. Experimentally observed narrow lines of the microresonators confirm the possibility of multiresonator quantum memory implementation.

DOI: 10.1103/PhysRevA.95.012338

I. INTRODUCTION

Control and manipulation of electromagnetic fields play a basic role in quantum information technologies [1]. In the past decade these matters have attracted a wave of interest among those working on quantum storage of single photon fields used as quantum information carriers [2–4]. Herein, quantum memory (QM) devices being experimentally elaborated seem to be key elements of the quantum computer [5–7] and the repeater [8] of long-distance quantum communication. The mainstream in current theoretical and experimental works on the QM creation is based on the usage of the resonant atomic ensembles as the robust keepers of a large amount of quantum data. The use of solid-state media, especially ensembles of the electron-nuclear-spin systems, is very promising for the creation of long-lived quantum storage. The rare-earth ions doped in inorganic crystals [9,10], nitrogen-vacancy centers in diamonds [11,12], and P donors in an isotopically pure Si crystal [13] can serve as such media, particularly for the use in microwave quantum storage [5,14–19].

The use of the photon echo approach [9,20] with the atomic system being in the high-Q single-mode resonator is considered especially promising for the practical implementation of multimode quantum storage. This happens due to the impedance matching enhancement of the resonant interaction of a weak-signal light field with a small number of atoms [21–26]. However, this impedance matching scheme has a limited spectral range, since its range is determined by the quality factor of the resonator [22,27,28].

In this paper we propose an approach providing broadband impedance matching QM. Instead of atomic ensembles (electron spins, etc.) in a single-mode resonator, in this approach [we call it the multiresonator (MR) QM approach], we use an array of high-Q single-mode microresonators located at the distance of a whole number of half wavelengths from each other and coupled to a broadband waveguide. The microresonator frequencies form a periodic structure that covers the broadband frequency range. The principle spatial scheme of the MR QM is depicted in Fig. 1.

It is worth noting that waveguide structures in which many microresonators are connected to the common waveguide [29] have been intensively studied in optics [30–32]. Great attention was paid to the structures consisting of microresonators with equal frequencies. In this case the realized nano-optical structures have demonstrated promising properties for the on-chip optical time delay lines [33]. We would also like to highlight various schemes in which optical waveguides are coupled with microresonators characterized by frequencies that are tunable within a wide spectral range [34] by using on-chip comb filters based on linear chirped fiber Bragg gratings (LCFBGs) [35–37], microring resonators [38,39], and cascaded Sagnac loop mirrors [40,41] (see also recent reviews in [42,43]). Here silica [44] and crystalline microresonators [45,46] are the most encouraging for quantum processing purposes due to their higher-quality factors. These optical integrated waveguide structures may also be useful for the implementation of the proposed MR QM.

We show that the MR scheme can be interesting for the universal quantum storage of a light field in a broadband frequency range. Here we find that perfect storage is possible at the optimal parameters of the microresonators and their coupling with the waveguide. The optimal parameters are determined by a single impedance matching condition for the interaction of a freely propagating light field with microresonators due to the fact that they form a spatial Bragg grating. We decided to call it the Bragg-type impedance matching condition.

Finally, we have constructed an experimental prototype of the studied MR QM in the microwave range that allowed us to localize the interaction within spatial size comparable to a few wavelengths and to implement independent control of the microresonator frequencies. Experimentally characterized

*samoi@yandex.ru

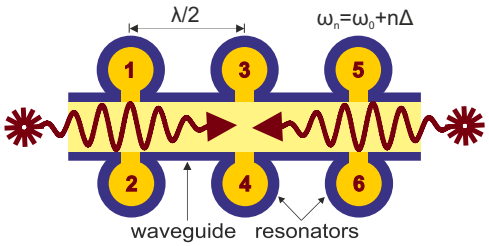

FIG. 1. Spatial scheme of the MR QM: 1–6 are single-mode microwave microresonators with distance $\lambda/2$ between the nearest ones; the microresonators contain dielectric insertions, which ensure the smallness of their spatial sizes in comparison with λ; and wavy lines represent the propagating electromagnetic fields interacting with the microresonators.

spectral properties of the prototype demonstrate its applicability for the studied QM.

II. PHYSICAL MODEL

In this section we give a theoretical study of the proposed QM scheme and analyze its basic properties.

A. Theoretical analysis

To simulate the interaction of a light field with an array of nearby microresonators in the broadband waveguide, we use the following multiparticle Tavis-Jaynes-Cummings-type model [47,48] with the Hamiltonian

$$\hat{H} = \int dk\, c|k|\hat{b}_k^\dagger \hat{b}_k + \sum_n [ck_0 + n\Delta]\hat{a}_n^\dagger \hat{a}_n + g\int dk \sum_n [e^{-ikzn}\hat{b}_k^\dagger \hat{a}_n + e^{ikzn}\hat{a}_n^\dagger \hat{b}_k], \quad (1)$$

where c is the speed of light; the integer index $n \in \{1,\ldots,N\}$ corresponds to the nth microresonator; the continuous index $k \in [-k_0-\delta_0;-k_0+\delta_0]\cup[k_0-\delta_0;k_0+\delta_0]$ corresponds to the forward and backward waveguide field modes located near the resonant frequency $\omega_0 = ck_0$; $\hat{a}_n, \hat{a}_n^\dagger$ and $\hat{b}_k, \hat{b}_k^\dagger$ are the annihilation and creation Bose operators of microresonator modes and of waveguide field modes, respectively; $z_n = zn$ is a spatial coordinate of the nth microresonator, where the nth microresonator has a frequency of $\omega_n = \omega_0 + \Delta n$; and Δ is the spectral distance between the nearest microresonator frequencies.

The first term in (1) corresponds to the energy (in the units $\hbar$) of the waveguide modes and the second term describes the energy of N microresonators. The third term in (1) corresponds to the interaction of the waveguide field with the microresonator modes, which is characterized by the coupling constant g. The point location of microresonators in (1) is provided by their contact localized coupling with a waveguide field, as shown in Fig. 1 (see also Fig. 6). We study the interaction of a single photon field with the analyzed compound MR system in the broadband waveguide. By taking into account the Hamiltonian (1), the wave function of this compound system has the following form:

$$|\psi\rangle = \left[\int dk\, f_k(t)\hat{b}_k^\dagger + \sum_n \alpha_n(t)\hat{a}_n^\dagger\right]|0\rangle, \quad (2)$$

where $f_k(t)$ and $\alpha_n(t)$ are the amplitudes of the waveguide and microresonator field modes that satisfy the normalization condition $\int dk\, f_k^*(t)f_k(t) + \sum_n \alpha_n^*(t)\alpha_n(t) = 1$.

By using the Schrödinger equation $(\partial_t + i\hat{H})|\psi\rangle = 0$, we get the following equations for the field amplitudes $f_k(t)$ and $\alpha_n(t)$:

$$\begin{aligned}[\partial_t + ic|k|]f_k(t) + ig\sum_n e^{-ikzn}\alpha_n(t) = 0,\\ [\partial_t + i\omega_0 + i\Delta n]\alpha_n(t) + ig\int dk\, e^{ikzn} f_k(t) = 0.\end{aligned} \quad (3)$$

The basic properties of MR QM can be easily studied for a retrieval stage. In this case, we assume that the waveguide mode stays in the vacuum state at time moment $t = 0$ when the MR system has absorbed an input single-photon field. This moment of time corresponds to the middle point between the absorption and retrieval stages. By substituting the formal solution $f_k(t) = -ig\int_0^t d\tau \sum_m e^{-i|k|[c(t-\tau)+\mathrm{sgn}(k)zm]}\alpha_m(\tau)$ in the second of Eqs. (3) and by replacing variables $\alpha_n(t) = e^{-i\omega_0 t}\beta_n(t)$, we get

$$[\partial_t + i\Delta n]\beta_n(t) + \frac{\pi g^2}{c}\sum_m e^{ik_0 z|n-m|}\beta_m(t-|n-m|z/c) = 0, \quad (4)$$

where we used the following initial conditions: $f_k(0) = 0$, $\beta_n(0) = c_n$, and $t \in [0; 2\pi/\Delta]$. In the case of a single microresonator ($n = 0$), we find the solution $\beta_0(t) = \exp\{-\Gamma t/2\}$, where $\Gamma = 2\pi g^2/c$ determines the mode linewidth. For a sufficiently narrow spectral width of an irradiated light pulse $|(n-m)z/c| \ll \delta t_s$ (where δt_s is the typical temporal duration of the pulse) and periodic spatial positions of microresonators $\{z = l\pi/k_0, l \in \mathbb{Z}\}$, we obtain the following solution:

$$\beta_n(t) = e^{-i\Delta nt}\left[c_n - \frac{\Gamma}{2\Delta}\left(1+\frac{\pi\Gamma}{2\Delta}\right)^{-1} \times \sum_m \frac{\sin[\Delta(n-m)t/2]}{(n-m)/2} e^{i\Delta(n-m)t/2}c_m\right], \quad (5)$$

where we introduced the variables $(-1)^{ln}\beta_n(t) \to \beta_n(t)$ and $(-1)^{ln}c_n \to c_n$.

The solution (5) demonstrates quite complex dynamics of the microresonator fields for arbitrary parameters of the interaction. Further, from Eq. (5) we find the quantum efficiency $\eta(t) = 1 - \sum_n |\beta_n(t)|^2$ of the field irradiation as the following product of two factors:

$$\begin{aligned}\eta(t) &= \eta_0(g)\eta_1(t),\\ \eta_0(g) &= \frac{2\pi\Gamma}{\Delta}\left[1+\frac{\pi\Gamma}{2\Delta}\right]^{-2},\\ \eta_1(t) &= \int_0^{\Delta t/(2\pi)} dv \left|\sum_n e^{-i2\pi nv}c_n\right|^2.\end{aligned} \quad (6)$$

First, we note that the solution (6) is time reversible and the quantum efficiency of the entire process is given by $\eta_{\text{total}} = \eta^2(T)$ (where $T = 2\pi/\Delta$). In this case, the temporal evolution of the system under consideration describes a storage of the input light pulse at the absorption stage (i.e., for $t < 0$). Second, as shown in Eq. (5), the input and output light pulses are identical to each other for the symmetric initial conditions $c_n^* = c_{-n}$, which means perfect fidelity for the retrieval of the input pulse. These two findings complete the analytic description of the studied MR QM scheme. The solutions (5) and (6) are the main analytic results of our work. Specific details of the calculation are given in the Appendix.

The studied quantum storage is valid for the light pulses with spectral width up to $\sim N\Delta$, which can be much larger in comparison with the linewidth Γ of a single microresonator mode. Below we analyze a condition for realization of highly efficient quantum storage.

B. Optimum condition and universality

The general properties and role of the impedance matching condition are well known in laser physics [49,50]. Recently, such conditions became important for the QM realization on atomic ensembles in a single-mode resonator [21,22,27,28] and for controlling the perfect light-atom quantum dynamics [17,51,52] in similar systems. The impedance condition physically adjusts the optimal interference effects of the light medium interaction in the resonant cavities that significantly facilitates the implementation of the main requirements to the quantum dynamics of light. Early experiments of the impedance matched photon echo QM schemes have been successfully demonstrated in optical cavities [23–25].

By using Eq. (6) we can analyze the condition of efficient light field irradiation. The temporal evolution of the irradiation is governed by the factor $\eta_1(t)$, which can be close to unity at time moment $t = 2\pi/\Delta$, as discussed in the next section. From the factor $\eta_0(g)$, we find that the maximum quantum efficiency [i.e., $\eta(T) = 1$] is reached under the following condition for the coupling constant g (or linewidth Γ of the microresonator mode) and spectral distance Δ between the microresonator frequencies:

$$\Delta = \frac{\pi}{2}\Gamma; \tag{7}$$

we call it the Bragg-type impedance matching condition providing the perfect MR QM operation.

As can be seen in Fig. 2, the quantum efficiency clearly depends on the dimensionless coupling constant $\tilde{g} = (\pi\Gamma/2\Delta)^{1/2} = g\pi/(c\Delta)^{1/2}$. We can experimentally control the values of g and Δ (see Sec. III), which facilitates the implementation of the condition (7). We also see in Fig. 2 that the efficiency $\eta_0(g)$ is higher than 90% in the interval $\tilde{g} \in [(\sqrt{10}-1)/3, (1+\sqrt{10})/3]$, in which it is possible to change the coupling constant in the range $\delta\tilde{g} \leqslant 2/3$. The variations of g and Δ show a stability of high efficiency. In turn, the fulfillment of the requirement $\eta_1(2\pi/\Delta) = 1$ for all the initial conditions of the microresonator states means that MR QM is universal within some spectral range (see also Appendix).

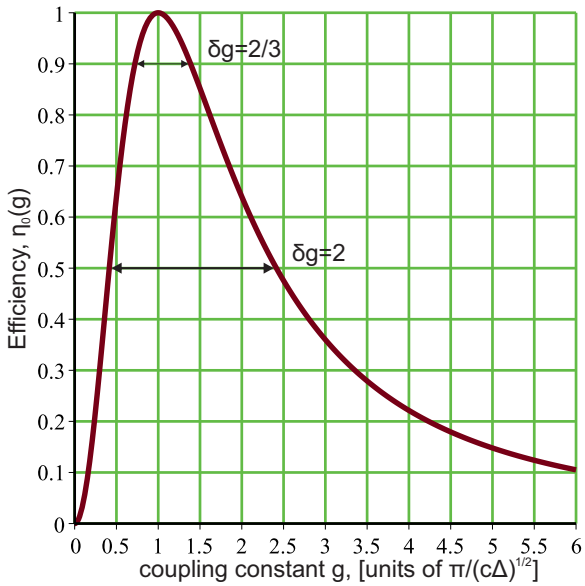

FIG. 2. Quantum efficiency $\eta_0 = 4\tilde{g}^2/(1+\tilde{g}^2)^2$ vs the dimensionless coupling constant $\tilde{g} = (\pi\Gamma/2\Delta)^{1/2}$; the maximum efficiency $\tilde{g} = 1$ corresponds to the Bragg-impedance matching condition.

For comparison, we also note that the usual impedance matching scheme based on using the atomic ensemble in a single-mode high-Q cavity [21–26] requires at least two impedance conditions (one of which is a spectral condition) for the quantum storage in a spectral width comparable to the linewidth of an empty cavity, as shown in a series of works [22,27,28]. However, it is sufficient to satisfy only one Bragg-type impedance condition (7) for implementation of perfect QM within an even broader spectral range in the considered scheme.

It is worth noting that the first scheme with a periodic spatial-frequency structure of resonant atomic lines was considered for optical QM in [53]. However, we have found that the pointlike spatial grating scheme can demonstrate the Bragg-type impedance matching condition for quantum storage in the broadband waveguide. That is, the impedance matching condition becomes possible due to the pointlike coupling of the light field with the microresonators forming a spatial grating (see Fig. 1). Herein, the spatial grating of the microresonators fulfills the role of a broadband distributed resonator for the light fields. Thus, any use of an additional (spectral) impedance matching condition is not necessary.

C. The MR QM dynamics

The MR scheme has a unique quality: The simple analytical solution (5) of the microresonator fields enables sustainable parametric control of all the memory characteristics. However, a detailed analysis of the dynamic structure of the QM schemes is a laborious fundamental problem for all multiparticle quantum systems and a general approach to this problem for the studied MR scheme is beyond the scope of the present paper.

Primarily, we focus on the important case of a short rectangular signal pulse when the initial data satisfy the

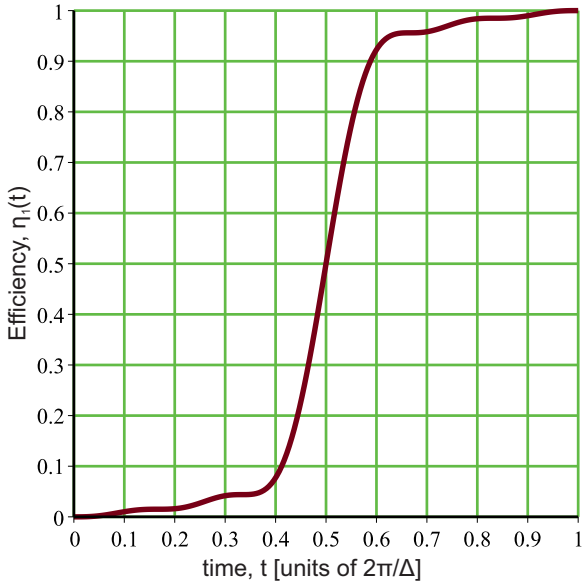

FIG. 3. Current efficiency $\eta_1(t)$ over time t in units of $2\pi/\Delta$ for $N = 6$. The time interval $t \in [0,\pi/\Delta]$ corresponds to half the storage phase.

condition $c_n = (-1)^n N^{-1/2}$ and the relation

$$\eta_1(2\pi u/\Delta) = \frac{1}{N}\int_0^u dv \left[\frac{\sin[N\pi(v-1/2)]}{\sin[\pi(v-1/2)]}\right]^2 \xrightarrow{N\to\infty} \theta(u-1/2) \quad (8)$$

is obtained for the factor $\eta_1(2\pi u/\Delta)$ of quantum efficiency (6), where $\theta(u)$ is a Heaviside step function [$\theta(0) = 1/2$]. The dynamic structure of QM behavior for $N = 6$ is determined by the curves in Figs. 3 and 4. The time interval $t \in [0,\pi/\Delta]$ corresponds to half the storage phase. We already see good enough light storage for $N = 6$. The envelope curve in Eq. (8) has a typical decay of the form e^{-Nu}, which provides a quite perfect storage phase for any $N > 6$. The maximum intensity $I_1(t)$ of the irradiated field is observed at $t = \pi/\Delta$. In this case, the current quantum efficiency of the field irradiation is given as $\eta_1(t) = \int_0^t dt\, I_1(t)/\int_0^\infty dt\, I_1(t)$ and, respectively, $I_1(t) = \partial_t \eta_1(t)$ [where we have used a normalization $\int_0^\infty dt\, I_1(t) = 1$ and Bragg-type impedance matching condition (7)]. Thus, all the energy stored initially in the microresonators will be irradiated eventually into the common waveguide. Herein, the minimum pulse duration of the signal pulses is limited by the value $\delta t_s \sim 2\pi/N\Delta$, which is determined by the total spectral width $N\Delta$ of the frequency comb structure, while shorter signal pulses will be out of the resonant interaction with the MR structure.

In turn, we can significantly increase the storage time by dynamic control of the spectral detunings between the microresonator modes after complete absorption of the input signal pulse. Namely, in accordance with Eq. (5), the evolution of each microresonator mode will be frozen for a given time interval T if all the microresonator frequencies are adiabatically aligned quickly with each other (i.e., $\Delta = 0$). Herein, the microresonator field modes will stay in the so-called nonradiative dark state during this time interval. However, after restoring the original frequencies, the behavior of the MR system is recovered and the emission of the recorded signal will be moved on the time interval T, as numerically demonstrated in Fig. 5 for a sufficiently high intrinsic quality factor of the microresonators $Q = \omega_0/2\gamma$, where $\gamma T \ll 1$ (see also the Appendix).

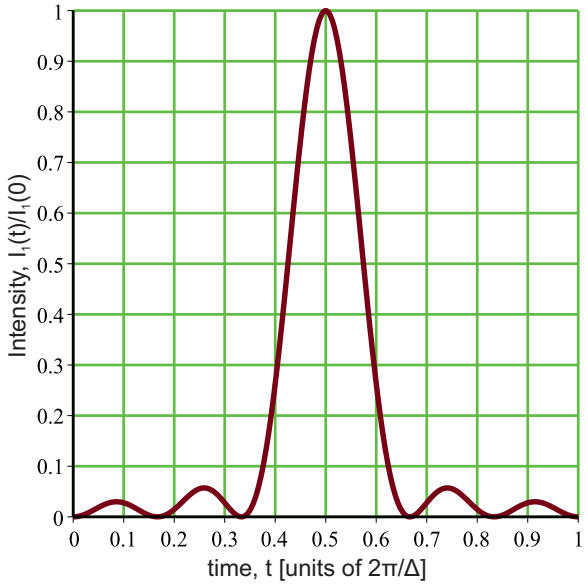

FIG. 4. Normalized intensity of echo pulse emission $I_1(t) = \partial_t \eta_1(t)$ as a function of time t in units of $2\pi/\Delta$ for $N = 6$; the pulse duration is about $\delta t_s \sim 2\pi/N\Delta$, which allows the use of short pulses.

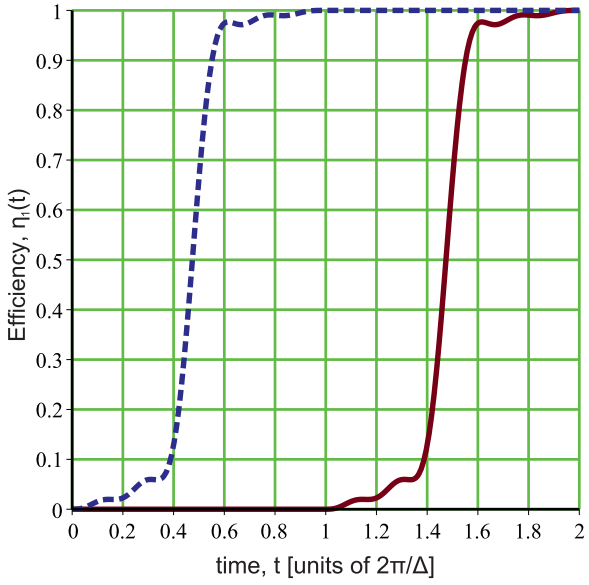

FIG. 5. Current efficiencies of the echo emission $\eta_1(t)$ over time t in units of $2\pi/\Delta$ for $N = 6$ at the matching condition (7). The blue dotted line shows the free evolution and the red solid line the evolution with increased lifetime of the stored pulse due to the alignment of the microresonator frequencies ($\Delta = 0$) during the time interval $T = 2\pi/\Delta$.

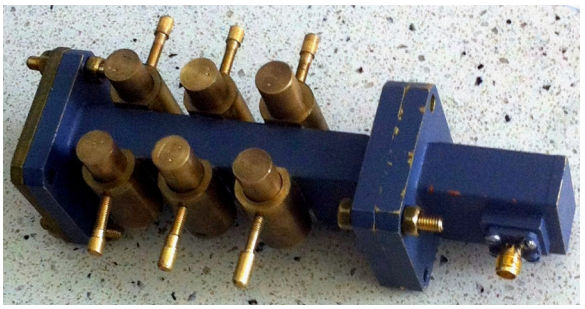

FIG. 6. Experimental prototype of the MR scheme: The waveguide is connected with six cylindric metallic resonators, the frequencies of which can be tuned using the handles fixing the lengths of the cylinders.

III. EXPERIMENTAL PROTOTYPE

For the implementation of the studied QM scheme, we have made an experimental prototype shown in Fig. 6 and we have measured its spectral characteristics on a network analyzer Agilent PNA-X. The prototype contains six cylindrical metallic resonators filled by the dielectric inserts characterized by the dielectric permittivity $\epsilon \sim 29$. Each resonator couples with the microwave waveguide through the thin slit. Our steady-state experiments have demonstrated the possibility of a sustainable precise control of the resonator frequencies in close proximity to each other. It was also observed that the controllable tuning of the resonant frequencies becomes complicated when the spectral distance Δ between the closest frequencies is less than 5 MHz. However, it was possible to perform almost independent tuning of each resonator frequency for larger spectral distance Δ.

Figure 7 shows three experimental curves demonstrating the periodically spaced frequencies of six closely situated compact resonators for three spectral detunings $\Delta = 5$–15 MHz with a total average linewidth $\Gamma_{\rm tot} = \Gamma + \gamma \approx 1.7$ MHz. We note that performing the experiments with varied spectral detuning Δ could provide an independent measurement of the constants Γ and γ and determine the constant g, respectively. The increase of the coupling constant g between the resonator and waveguide field modes usually leads to higher values of the parameters Γ and γ. However, in some range of changes, it is possible to vary g and Γ, respectively, without significant changes of γ, as was experimentally observed in the studied prototype. It is obvious that a small decay constant γ determines almost exponential decay of the quantum efficiency (i.e., $\eta \sim e^{-4\pi\gamma/\Delta}$).

As can be seen from a comparison of the curves in Fig. 7, the realized MR prototype can be configured for different spectral distances between the closest frequencies. The tunable control of the spectral lines is achieved by the appropriate change of the geometric dimensions of the cylindrical resonators without variation of any other parameters. However, the frequency of each resonator mode in Fig. 7 can be significantly shifted by the interaction with the field modes of other resonators via the interaction with the common waveguide field. We observed this effect in experiments with two nearest resonator modes. The frequency shift of one resonator mode visibly changed the frequency of another mode for sufficiently small

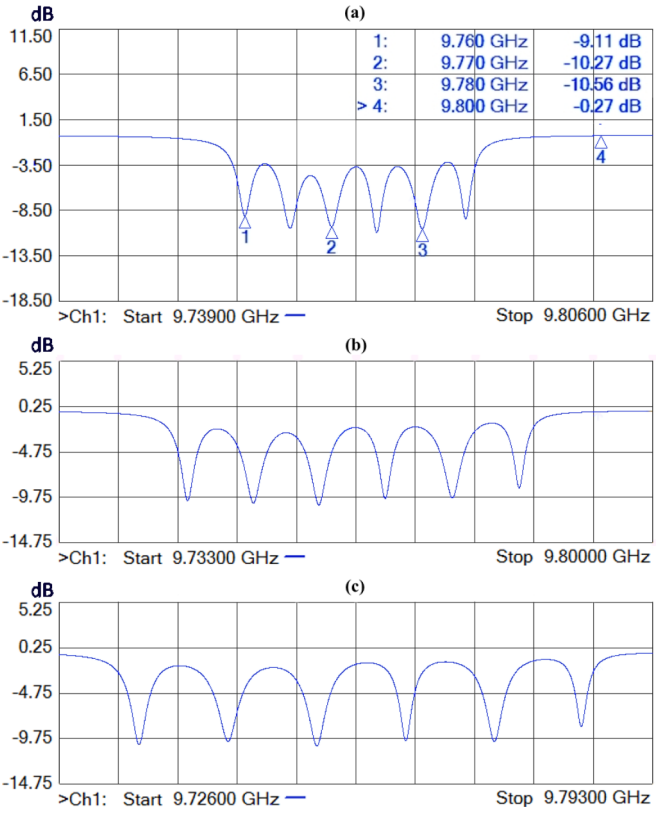

FIG. 7. Controllable frequency spectrum of resonator lines in logarithmic scale: The distance Δ between the closest frequencies is (a) 5 MHz, (b) 10 MHz, and (c) 15 MHz.

spectral distance between these modes (i.e., for $\Delta \sim \Gamma_{\rm tot}$). In this spectral range the two frequencies started to get closer to each other, experiencing some extra attraction due to their interaction via the waveguide field. That, in our opinion, indicated the value of $\Gamma \gtrsim \gamma$.

Thus, the prototype of MR QM has demonstrated some of the basic properties required for implementing the storage of microwave electromagnetic fields. At the same time, the Bragg-type impedance matching condition (7) requires the creation of the periodic frequency combs with a smaller frequency interval Δ in comparison with the detunings depicted in Fig. 7. Such a frequency setting requires an experimental system providing precise control of the closely situated resonator frequencies. This is a subject for further study.

We can also apply the currently being elaborated methods of fast switching of the resonator frequencies [54–59] (see also reviews in [42,43,60]) for implementation of longer storage and on-demand retrieval of the absorbed microwave fields. These methods can work with switching time on the order of 100 ns, which is applicable in our scheme. In addition, the quantum storage in the microwave spectrum region [15] requires perfect control of MR QM parameters and a fairly low temperature (around 10^{-2} K) that is necessary for protecting against microwave quantum noises, which are a topic of our current investigation.

IV. CONCLUSION

We have studied the system of high-Q microresonators that have a pointlike coupling with a broadband waveguide

(MR scheme). The aim of this study is to identify and demonstrate the optical conditions under which the MR scheme can ensure high quantum efficiency during the storage and readout of the broadband microwave fields. Herein, the microresonators form a spatial Bragg grating system and a periodic structure of narrow resonance lines. We have obtained an analytical solution (5) describing the quantum dynamics of the microresonator fields. Based on this solution, we have found a single type of impedance matching condition (7) (we called it the Bragg-type impedance matching condition) providing perfect storage and retrieval of the microwave light fields in the MR system. The proposed MR QM scheme is interesting because it allows us to work with the broadband microwave fields using a system of high-Q microresonators. Due to the high-Q factor, it is possible to significantly enhance the interaction of the microwave fields with the individual microresonators as well as with the systems of electronic spins that could be in these microresonators. Such a MR scheme will greatly facilitate the practical implementation of broadband QM devices.

The MR scheme can be implemented by employing different physical platforms: for example, using planar microwave waveguides characterized by highly reduced spatial sizes, various nano-optical waveguide structures, photonic crystals, and other systems that allow localized interactions of many quantum objects with a broadband carrier of signals. In particular, it seems useful to apply the nano-optical waveguides integrated with microcavities and LCFBGs (see [29,34,37]). Herein, it is necessary to satisfy the Bragg-type impedance matching condition (7) and to achieve a sufficiently high intrinsic quality factor of microcavity modes. In turn, the fast frequency switching of the optical microcavities can be operated by electro-optics and free-carrier dispersion control [61].

The proposed MR scheme has been experimentally constructed in a microwave prototype (see Fig. 6). In this prototype, we have obtained a spatial localization of many compact composite resonators coupled to a common typical microwave waveguide. In addition to that, we have performed controlled tuning of the resonator frequencies and have created a periodic frequency structure (see Fig. 7) required for broadband quantum storage. The constructed prototype has promising technical properties—compactness, low cost, and ease of fabrication—which are convenient for controlling the field dynamics and integration into quantum circuits.

It is worth noting that the proposed MR scheme and its prototype provide individual control of each microresonator, which is promising for fast quantum processing with photonic qubits. In particular, the broadband character and presence of many interacting local quantum subsystems in these schemes seem useful to generate and study entangled states in multiparticle quantum systems [62–64].

ACKNOWLEDGMENTS

This research was supported by the Russian Government Program of Competitive Growth of Kazan Federal University and by the Russian Foundation for Basic Research through Grant No. 15-42-02462.

APPENDIX: CALCULATION OF EFFICIENCY

After the Laplace transformation $x_n(p) = \int_0^\infty dt\, e^{-pt}\beta_n(t)$, from Eq. (4) we get

$$[p + i\Delta n + \gamma]x_n(p) + \frac{\Gamma}{2}\sum_m e^{(ik_0 z - pz/c)|n-m|}x_m(p) = c_n, \tag{A1}$$

where γ is a small decay factor that was previously omitted for simplicity and $\Gamma = 2\pi g^2/c$. Assuming a sufficiently narrow spectral width of an irradiated pulse $|n-m|pz/c \ll 1$ in (A1) and using a spatial condition $\{z = l\pi/k_0, l \in \mathbb{Z}\}$ of microresonators, we obtain

$$x_n(p) = \frac{1}{p + i\Delta n + \gamma}\left[c_n - \frac{\Gamma}{2Q(p)}\sum_m \frac{c_m}{p + i\Delta m + \gamma}\right],$$
$$Q(p) = 1 + \frac{\Gamma}{2}\sum_n \frac{1}{p + i\Delta n + \gamma}, \tag{A2}$$

where we introduce variables $(-1)^{ln}x_n(p) \to x_n(p)$ and $(-1)^{ln}c_n \to c_n$.

From Eq. (A2) we have $\sum_n [p + i\Delta n + \gamma]^{-1} = \pi/\Delta$ for a large number of the microresonators $N \gg 1$ and

$$x_n(p) = \frac{1}{p + i\Delta n + \gamma} \times \left[c_n - \frac{\Gamma}{2}\left(1 + \frac{\pi\Gamma}{2\Delta}\right)^{-1}\sum_m \frac{c_m}{p + i\Delta m + \gamma}\right], \tag{A3}$$

which allows us to correctly recover the dynamics of the microresonator modes only for the time interval we are interested in $t \in [-T; T]$ $(T = 2\pi/\Delta)$. Hence, assuming a high intrinsic quality factor of microresonators $\gamma \ll 1/T$ and applying the inverse Laplace transformation, we have (5). It is important to note that numerical calculations show that the solution can also be used for a small N. For example, for $N = 4$, the difference between the numerical solution and the solution of (5) is less than 1%.

Further, from (4) for quantum efficiency $\eta(t) = 1 - \sum_n |\alpha_n(t)|^2$ we have

$$\eta(t) = 1 - \sum_n |\beta_n(t)|^2 = \Gamma\int_0^t d\tau \left|\sum_n \beta_n(\tau)\right|^2, \tag{A4}$$

where with (5) we easily get (6). Since for all initial data the normalization condition is $\sum_n |c_n|^2 = 1$, the following relation is true:

$$\eta_1(2\pi/\Delta) = \int_0^1 dv \sum_{n,m} e^{i2\pi(n-m)v}c_n^* c_m = \sum_n |c_n|^2 + \sum_{n,m}^{n\neq m}\frac{e^{i2\pi(n-m)} - 1}{i2\pi(n-m)}c_n^* c_m = \sum_n |c_n|^2 = 1, \tag{A5}$$

which proves the universality of MR QM.

[1] G. Kurizki, P. Bertet, Y. Kubo, K. Mølmer, D. Petrosyan, P. Rabl, and J. Schmiedmayer, Proc. Natl. Acad. Sci. USA **112**, 3866 (2015).

[2] A. I. Lvovsky, B. C. Sanders, and W. Tittel, Nat. Photon. **3**, 706 (2009).

[3] K. Hammerer, A. S. Sørensen, and E. S. Polzik, Rev. Mod. Phys. **82**, 1041 (2010).

[4] C. Simon *et al.*, Eur. Phys. J. D **58**, 1 (2010).

[5] C. Grezes, B. Julsgaard, Y. Kubo, W. L. Ma, M. Stern, A. Bienfait, K. Nakamura, J. Isoya, S. Onoda, T. Ohshima, V. Jacques, D. Vion, D. Esteve, R. B. Liu, K. Mølmer, and P. Bertet, Phys. Rev. A **92**, 020301 (2015).

[6] M. Mariantoni, H. Wang, T. Yamamoto, M. Neeley, R. C. Bialczak, Y. Chen, M. Lenander, E. Lucero, A. D. O'Connell, D. Sank, M. Weides, J. Wenner, Y. Yin, J. Zhao, A. N. Korotkov, A. N. Cleland, and J. M. Martinis, Science **334**, 61 (2011).

[7] C. D. Hill, E. Peretz, S. J. Hile, M. G. House, M. Fuechsle, S. Rogge, M. Y. Simmons, and L. C. L. Hollenberg, Sci. Adv. **1**, e1500707 (2015).

[8] N. Sangouard, C. Simon, H. de Riedmatten, and N. Gisin, Rev. Mod. Phys. **83**, 33 (2011).

[9] W. Tittel, M. Afzelius, T. Chaneliére, R. Cone, S. Kröll, S. Moiseev, and M. Sellars, Laser Photon. Rev. **4**, 244 (2009).

[10] M. Zhong, M. P. Hedges, R. L. Ahlefeldt, J. G. Bartholomew, S. E. Beavan, S. M. Wittig, J. J. Longdell, and M. J. Sellars, Nature (London) **517**, 177 (2015).

[11] G. D. Fuchs, G. Burkard, P. V. Klimov, and D. D. Awschalom, Nat. Phys. **7**, 789 (2011).

[12] P. C. Maurer, G. Kucsko, C. Latta, L. Jiang, N. Y. Yao, S. D. Bennett, F. Pastawski, D. Hunger, N. Chisholm, M. Markham, D. J. Twitchen, J. I. Cirac, and M. D. Lukin, Science **336**, 1283 (2012).

[13] J. J. L. Morton, A. M. Tyryshkin, R. M. Brown, S. Shankar, B. W. Lovett, A. Ardavan, T. Schenkel, E. E. Haller, J. W. Ager, and S. A. Lyon, Nature (London) **455**, 1085 (2008).

[14] Y. Kubo, C. Grezes, A. Dewes, T. Umeda, J. Isoya, H. Sumiya, N. Morishita, H. Abe, S. Onoda, T. Ohshima, V. Jacques, A. Dréau, J.-F. Roch, I. Diniz, A. Auffeves, D. Vion, D. Esteve, and P. Bertet, Phys. Rev. Lett. **107**, 220501 (2011).

[15] S. Probst, H. Rotzinger, S. Wünsch, P. Jung, M. Jerger, M. Siegel, A. V. Ustinov, and P. A. Bushev, Phys. Rev. Lett. **110**, 157001 (2013).

[16] B. Julsgaard, C. Grezes, P. Bertet, and K. Mølmer, Phys. Rev. Lett. **110**, 250503 (2013).

[17] K. I. Gerasimov, S. A. Moiseev, V. I. Morosov, and R. B. Zaripov, Phys. Rev. A **90**, 042306 (2014).

[18] C. Grezes, B. Julsgaard, Y. Kubo, M. Stern, T. Umeda, J. Isoya, H. Sumiya, H. Abe, S. Onoda, T. Ohshima, V. Jacques, J. Esteve, D. Vion, D. Esteve, K. Mølmer, and P. Bertet, Phys. Rev. X **4**, 021049 (2014).

[19] D. O. Krimer, M. Zens, S. Putz, and S. Rotter, Laser Photon. Rev. **10**, 1023 (2016).

[20] S. A. Moiseev and S. Kröll, Phys. Rev. Lett. **87**, 173601 (2001).

[21] M. Afzelius and C. Simon, Phys. Rev. A **82**, 022310 (2010).

[22] S. A. Moiseev, S. N. Andrianov, and F. F. Gubaidullin, Phys. Rev. A **82**, 022311 (2010).

[23] M. Sabooni, Q. Li, S. Kröll, and L. Rippe, Phys. Rev. Lett. **110**, 133604 (2013).

[24] M. Sabooni, S. T. Kometa, A. Thuresson, S. Kröll, and L. Rippe, New J. Phys. **15**, 035025 (2013).

[25] P. Jobez, I. Usmani, N. Timoney, C. Laplane, N. Gisin, and M. Afzelius, New J. Phys. **16**, 083005 (2014).

[26] T. Chanelière, Opt. Express **22**, 4423 (2014).

[27] S. A. Moiseev, Phys. Rev. A **88**, 012304 (2013).

[28] E. S. Moiseev and S. A. Moiseev, J. Mod. Opt. **63**, 2081 (2016).

[29] J. S. Foresi, P. R. Villeneuve, J. Ferrera, E. R. Thoen, G. Steinmeyer, S. Fan, J. D. Joannopoulos, L. C. Kimerling, H. I. Smith, and E. P. Ippen, Nature (London) **390**, 143 (1997).

[30] S. V. Boriskina, in *Photonic Microresonator Research and Applications*, edited by I. Chremmos, O. Schwelb, and N. Uzunoglu (Springer, Boston, 2010), pp. 393–421.

[31] F. Morichetti, C. Ferrari, A. Canciamilla, and A. Melloni, Laser Photon. Rev. **6**, 74 (2012).

[32] W. Bogaerts, P. De Heyn, T. Van Vaerenbergh, K. De Vos, S. Kumar Selvaraja, T. Claes, P. Dumon, P. Bienstman, D. Van Thourhout, and R. Baets, Laser Photon. Rev. **6**, 47 (2012).

[33] F. Xia, L. Sekaric, and Y. Vlasov, Nat. Photon. **1**, 65 (2007).

[34] R. E. Saperstein, N. Alic, S. Zamek, K. Ikeda, B. Slutsky, and Y. Fainman, Opt. Express **15**, 15464 (2007).

[35] I. Giuntoni, P. Balladares, R. Steingrüber, J. Bruns, and K. Petermann, *Optical Fiber Communication Conference/National Fiber Optic Engineers Conference 2011* (Optical Society of America, Washington, DC, 2011), p. OThV3.

[36] M. W. Pruessner, T. H. Stievater, M. S. Ferraro, and W. S. Rabinovich, Opt. Express **15**, 7557 (2007).

[37] M. W. Pruessner, T. H. Stievater, and W. S. Rabinovich, Opt. Lett. **32**, 533 (2007).

[38] P. Dong, S. F. Preble, and M. Lipson, Opt. Express **15**, 9600 (2007).

[39] B. G. Lee, A. Biberman, P. Dong, M. Lipson, and K. Bergman, IEEE Photon. Technol. Lett. **20**, 767 (2008).

[40] X. Sun, L. Zhou, J. Xie, Z. Zou, L. Lu, H. Zhu, X. Li, and J. Chen, Opt. Lett. **38**, 567 (2013).

[41] X. Jiang, J. Wu, Y. Yang, T. Pan, J. Mao, B. Liu, R. Liu, Y. Zhang, C. Qiu, C. Tremblay, and Y. Su, Opt. Express **24**, 2183 (2016).

[42] M. J. R. Heck, J. F. Bauters, M. L. Davenport, J. K. Doylend, S. Jain, G. Kurczveil, S. Srinivasan, Y. Tang, and J. E. Bowers, IEEE J. Sel. Top. Quantum Electron. **19**, 6100117 (2013).

[43] H. Du, F. S. Chau, and G. Zhou, Micromachines **7**, 69 (2016).

[44] P.-H. Wang, J. A. Jaramillo-Villegas, Y. Xuan, X. Xue, C. Bao, D. E. Leaird, M. Qi, and A. M. Weiner, Opt. Express **24**, 10890 (2016).

[45] V. S. Ilchenko, A. A. Savchenkov, A. B. Matsko, and L. Maleki, Phys. Rev. Lett. **92**, 043903 (2004).

[46] I. S. Grudinin and N. Yu, Optica **2**, 221 (2015).

[47] E. T. Jaynes and F. W. Cummings, Proc. IEEE **51**, 89 (1963).

[48] M. Tavis and F. W. Cummings, Phys. Rev. **170**, 379 (1968).

[49] H. A. Haus, *Waves and Fields in Optoelectronics* (Prentice-Hall, Englewood Cliffs, 1984).

[50] A. E. Siegman, *Lasers* (University Science Books, Mill Valley, 1986).

[51] A. Kalachev and O. Kocharovskaya, Phys. Rev. A **88**, 033846 (2013).

[52] V. V. Kuz'min, A. N. Vetlugin, and I. V. Sokolov, Opt. Spectrosc. **119**, 1004 (2015).

[53] M. Tian, D. Vega, and J. Dilles, Phys. Rev. A **87**, 042338 (2013).

[54] X. Liu, L. P. B. Katehi, W. J. Chappell, and D. Peroulis, J. Microelectromech. Syst. **19**, 774 (2010).
[55] M. Sandberg, C. M. Wilson, F. Persson, T. Bauch, G. Johansson, V. Shumeiko, T. Duty, and P. Delsing, Appl. Phys. Lett. **92**, 203501 (2008).
[56] H. Joshi, H. H. Sigmarsson, D. Peroulis, and W. J. Chappell, *2007 IEEE/MTT-S International Microwave Symposium* (IEEE, Piscataway, 2007), pp. 2133–2136.
[57] R. Stefanini, J. D. Martinez, M. Chatras, A. Pothier, V. E. Boria, and P. Blondy, IEEE Microwave Wireless Components Lett. **21**, 237 (2011).
[58] M. Goryachev and M. E. Tobar, J. Appl. Phys. **118**, 204504 (2015).
[59] T. Brecht, M. Reagor, Y. Chu, W. Pfaff, C. Wang, L. Frunzio, M. H. Devoret, and R. J. Schoelkopf, Appl. Phys. Lett. **107**, 192603 (2015).
[60] R. R. Mansour, IEEE Microwave Mag. **10**, 84 (2009).
[61] A. Melloni, A. Canciamilla, C. Ferrari, F. Morichetti, L. O'Faolain, T. F. Krauss, R. D. L. Rue, A. Samarelli, and M. Sorel, IEEE Photon. J. **2**, 181 (2010).
[62] S. Maniscalco, F. Francica, R. L. Zaffino, N. Lo Gullo, and F. Plastina, Phys. Rev. Lett. **100**, 090503 (2008).
[63] S. Bougouffa and Z. Ficek, J. Phys. B **46**, 224006 (2013).
[64] S. Dooley, F. McCrossan, D. Harland, M. J. Everitt, and T. P. Spiller, Phys. Rev. A **87**, 052323 (2013).